Bioinorganic Chemistry

DOI: 10.1002/anie.201102582

Discovery of Catalytic Peptides for Inorganic Nanocrystal Synthesis by a Combinatorial Phage Display Approach**

*Zengyan Wei, Yoshiaki Maeda, and Hiroshi Matsui**

Nature tends to find the easiest way to grow materials with high efficiency and selectivity at room temperature, and thus a biomimetic approach is a potential pathway to synthesize inorganic nanocrystals at room temperature since enzymes can catalyze the growth of materials into desired structures at low temperature. Recently, several promising peptides and proteins were demonstrated to catalyze the growth of semiconductors;[1] however, the successful discovery of the catalytic peptide sequences needed to go through trial-and-error processes[2] and thus the development of a systematic method with combinatorial selection would be desirable for the future development of materials. Here, we report a novel evolutionary approach to identify catalytic peptides for the room-temperature growth of target semiconductor materials. The conventional phage display technique is limited to finding peptide sequences that bind specific target surfaces; however, our combinatorial phage display approach directly screens peptides that catalyze the growth of the target material. The unique feature of this technique is that the panning of peptides takes place in precursor solutions where no reactions are expected to occur without catalysts. Thus, the product is observed only when there are phages in the solution that display peptides that catalyze the target reactions. The use of our method provided a simple and convenient route to discover a catalytic peptide for the growth of ZnO nanocrystals at room temperature, which conventional synthetic methods cannot match. The method is expected to have a wide application since this novel screening method could be used to generate a wide range of new catalysts.

Biomineralizing peptides that catalyze the growth of metal nanocrystals have previously been isolated from tissues and cells of animals and microorganisms.[3] However, a broad range of materials cannot be generated by peptides since there is no combinatorial method to determine the specific sequences of the catalytic peptides.

Recently, an in vivo combinatorial biological protocol was utilized to screen peptides that exhibit selectivity for binding particular inorganic surfaces.[4] Since these peptides cap specific crystalline faces of target materials, some of these peptides happen to mediate the formation of specific inorganic nanoparticles. However, a critical drawback still exists in that the selected peptides do not necessarily catalyze the nucleation of nanocrystals at low temperature, and in many cases the selected peptides only influence the shape and the structure of the resulting nanocrystals.[4b,5] Therefore, it is desirable to establish a simple method for the combinatorial selection of catalytic peptides to grow semiconductor nanocrystals at room temperature for the engineering of future materials. The use of the biopanning process in the growth medium allows the catalytic peptides to be isolated directly from the semiconductor growth solution. Our method enabled the peptide to be identified that nucleated zinc oxide (ZnO) nanoparticles at room temperature through a nonclassical crystallization path.[6] The majority of important oxide semiconductor nanocrystals for solar cells, microelectronics, medical imaging, data storage, and sensors are grown at high temperature, and the low-temperature synthesis will be effective in reducing the energy consumption in manufacturing processes thereby reducing the production cost, the facility size (such as cooling systems), and the manpower.[1b] Our method provides a simple and convenient route for the discovery of biomineralizing peptides for a variety of inorganic nanocrystals at room temperature.

In the proof-of-concept study, the combinatorial approach was used to investigate the growth of ZnO nanoparticles. ZnO is a useful large band gap semiconductor material, which has widely been applied in solar cells, gas sensors, ultraviolet nanolasers, and blue light-emitting diodes (LEDs).[7] As illustrated in Figure 1, the phages were first incubated with the zinc precursor (10 mg mL^{-1} zinc nitrate solution) at room temperature (steps a and b). Phage viruses have on the order of 10^{11} random peptide sequences. If some of these phages catalyze the growth of ZnO nanocrystals (step c) through their displayed peptides, they can be recovered from the solution by a simple centrifuge method (step d). The nanocrystals grown on the viruses were confirmed as crystalline ZnO by transmission electron microscopy (TEM) and selected-area electron diffraction (SAED; see also the Supporting Information). After removal of unbound phages by extensive washing with a 0.1% aqueous solution of Tween 20, the residual phage viruses were released from the ZnO with a 0.2 M glycine/HCl solution at pH 2.2, and then the eluted phage viruses were amplified (step e). After three

[*] Z. Wei, Dr. Y. Maeda, Prof. H. Matsui
Department of Chemistry and Biochemistry
City University of New York-Hunter College
695 Park Avenue, New York, NY 10065 (USA)
E-mail: hmatsui@hunter.cuny.edu

[**] This work was supported the U.S. Department of Energy, Office of Basic Energy Sciences, Division of Materials Sciences and Engineering under Award No. DE-FG-02-01ER45935. The Hunter College infrastructure is supported by the National Institutes of Health, the RCMI program (G12-RR003037-245476). Z.W. and Y.M. equally contributes to this work. Y.M. thanks the International Training Program provided through Tokyo University of Agriculture and Technology (TUAT) and Japan Society for the Promotion of Science (JSPS).

Supporting information for this article is available on the WWW under http://dx.doi.org/10.1002/anie.201102582.

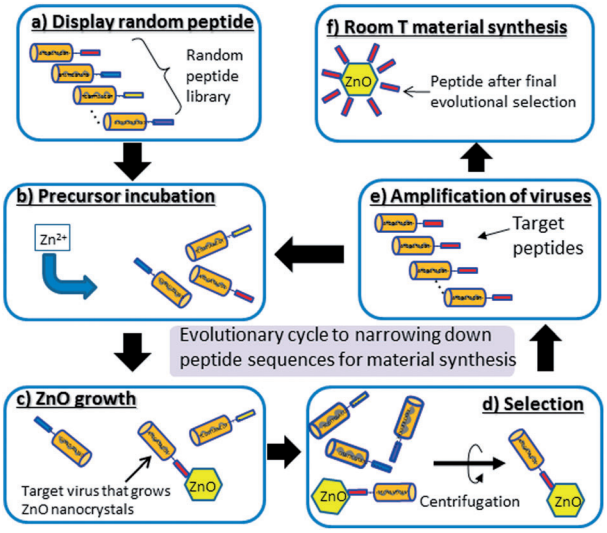

Figure 1. Scheme of the proposed evolutionary synthesis of ZnO by discovering catalytic peptides that can grow ZnO at room temperature.

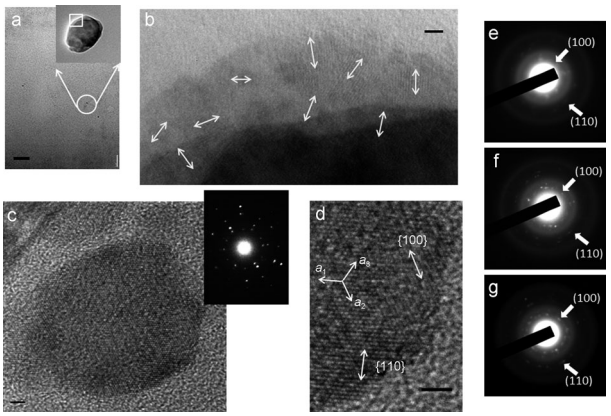

Figure 2. Microscopy studies on the mineralization process. a) TEM image of ZnO nanoparticles after 4 days incubation in the precursor solution for peptide growth, scale bar = 1 μm. Inset: Magnified image of the circled area. b) HRTEM image of the square region in (a), showing nanoparticle domains with (100) faces (white arrows) oriented in random directions. Scale bar = 2 nm. c) TEM image of ZnO nanocrystals after 3 weeks incubation in the precursor solution for peptide growth. Inset: NBED pattern of this nanocrystal showing the single crystallinity, with a [0001] transmission direction. For details see the diffraction pattern indexation in Figure S3 of the Supporting Information. Scale bar = 2 nm. d) HRTEM image of (c) resolving (100) and (110) faces (shown by arrows). Scale bar = 2 nm. e) SAED pattern for ZnO nanoparticles after incubation for 12 hours in the precursor solution for peptide growth. f) SAED pattern for ZnO nanoparticles after 4 days incubation in the precursor solution for peptide growth. g) SAED pattern for ZnO nanoparticles after 3 weeks incubation in the precursor solution for peptide growth. In (e)–(g), the (100) and (110) faces are shown by arrows.

rounds of selection, the peptide sequences displayed on the phage viruses were analyzed to identify the catalytic peptides (step f). This resulted in one peptide, ZP-1 (GAMHLPWHMGTL), being identified. Careful selection of the Zn precursors (in step b) is important for this method. If conventional Zn precursors that form zinc hydroxide solids in aqueous solution are used, amorphous $Zn(OH)_x$ might grow in addition to ZnO nanoparticles in the phage solution, and then the panning process could also contain the sequences of peptides that bind amorphous $Zn(OH)_x$ nanoparticles. It should also be noted that our method has an advantage of reducing the number of nontargeted phages accidently contained in the final selection because viruses free of inorganic nanoparticles are less likely to be collected by centrifugation because of their significantly lower mass.[8]

Next, to confirm whether the selected peptide can catalyze the crystallization without virus templates, we incubated ZP-1 peptide ($50\ mg\,mL^{-1}$) with the same zinc precursors ($10\ mg\,mL^{-1}$) for four days. After purifying the mixture three times by centrifugation, polydispersed particles with diameters of 20–100 nm were observed in the TEM image (Figure 2a). A control experiment without the peptides resulted in no nanoparticles growing, thus demonstrating that the ZP-1 peptide plays a critical role in the nucleation and the catalytic growth of the crystal. A high-resolution TEM (HRTEM) image of the circled area in the inset of Figure 2a shows multiple crystalline domains with diameters less than 5 nm (Figure 2b). The *d* spacing of this single-crystal domain was determined to be (2.82 ± 0.05) Å, which corresponds to the (100) lattice fringe of wurtzite ZnO. SAED patterns further confirmed the single-crystalline nature of this domain (Figure 2f and see Figure S3b in the Supporting Information) and the *d* spacings of $a = 0.325$ nm and $c = 0.521$ nm agree with the wurtzite structure of ZnO (JCPDS card no. 36-1451). The energy-dispersive X-ray (EDX) spectrum, which shows nearly pure compositions of zinc and oxygen, also supports the formation of ZnO nanocrystals from the catalytic ZP-1 peptide (see Figure S2 in the Supporting Information). Of the 100 samples studied, 86% of the nanoparticles in the samples were found to have a wurtzite structure.

The crystallization of ZnO on the catalytic ZP-1 peptide was studied by monitoring the ZnO particles by TEM and SAED over time. As the mineralization time increased, the evolution of crystallinity could be observed by changes in the SAED patterns, with the development of (100) and (110) faces evident after mixing the ZP-1 peptide with the zinc precursor (Figure 2e–g), thus indicating that the directions of growth are along $\langle 01\bar{1}0\rangle$ and $\langle 11\bar{2}0\rangle$. Reports of the growth of ZnO crystals along these directions are rare, especially at low temperature, because the growth along the [0001] axis is usually much faster than in the other directions.[9] It was reported previously that ZnO tends to grow along unusual directions corresponding to the nonpolar crystalline faces when insufficient growth medium is available.[10] Since both (100) and (110) are nonpolar faces,[11] we attribute the growth of ZnO along $\langle 01\bar{1}0\rangle$ and $\langle 11\bar{2}0\rangle$ to a slow diffusion of zinc ions towards the peptide surfaces,[3] which would create the condition of insufficient growth medium. In addition, charged groups of the ZP-1 peptide could preferentially attach to polar crystalline faces such as (001) and $(00\bar{1})$,[11] and as a result the anisotropic growth along these directions could be quenched.

Previously, peptide-assisted aggregation-driven crystal fusion by the nonclassical crystallization path was observed in the growth of other nanocrystals,[12] and a similar fusing process also occurs in the peptide-catalyzed growth of ZnO nanocrystals. When the morphologies of ZnO nanocrystals are compared after 4 days and 3 weeks, the HRTEM images (Figure 2b and d) indicate that the primitive crystalline domains of ZnO become fused in the anisotropic direction to form larger single-crystalline domains as the incubation time is increased. In Figure 2b, the crystalline domains with a diameter of 5 nm are randomly oriented in the sample after four days of incubation. However, after three weeks these domains are aligned and fused on {100} to form a larger single-crystalline domain (Figure 2d). Subtle short-range order of the domains along {110} is also evident. These observations indicate that the fusion of primitive nanoparticles mainly occurs along {100}. The diffraction spots in the SAED pattern of the sample after three weeks of incubation (Figure 2g) are attenuated, except for (100) and (110), compared to the pattern recorded after four days of incubation (Figure 2f); this finding is consistent with the HRTEM result. Analysis of the structure of the ZnO single nanoparticle after three weeks by nanobeam electron diffraction (NBED; inset of Figure 2c) reveals the single crystallinity induced by the anisotropic fusion of the nanocrystalline domains.

Metal nanoparticles have previously been observed to coagulate into larger particles by photomediation.[13] The driving force could be the induced electromagnetic field around the excited particles,[13b] while the redistribution of ligands and ions on the particle surfaces could also allow anisotropic growth.[13a] Extended structures from oriented nanoparticles can also be formed by dipole moments that drive the fusion of nanoparticles on high-energy faces.[14] However, in this case, the fusion of semiconductor nanoparticles occurs on nonpolar crystalline faces that are rarely observed.[12] Our results suggest that the ZP-1 peptide can not only nucleate the catalytic growth of semiconductor nanoparticles, but can also induce the anisotropic coagulation of primitive crystalline domains at room temperature to form single-crystalline nanoparticles easily and without the need to add complex capping reagents.[15]

In conclusion, a novel evolutionary protocol has been established to discover catalytic peptides for the synthesis of new materials at low temperature. We succeeded in synthesizing single-crystalline ZnO nanocrystals at room temperature by using the catalytic peptide discovered by this combinatorial technique. This combinatorial phage display approach led to the discovery of the ZP-1 peptide, which displayed strong catalytic activity for the growth of ZnO nanocrystals at room temperature.

Experimental Section

Combinatorial peptide display: The Ph.D.-12 phage display peptide library kit (New England Bio Labs, Beverly, MA) was used to select ZnO-mineralizing peptides. The phage library (10^{11} pfu) was mixed with $Zn(NO_3)_2$ solution (10 mg mL^{-1}, 300 μL) and incubated for 4–6 days at room temperature. The resulting nanocrystals were recovered by centrifugation (18000 × *g*, 30 min), and then washed with deionized water containing 0.1% Tween 20 (3 × 1 mL). The phages were eluted from the nanocrystals by the addition of 0.2 M glycine/HCl (pH 2.2) over 20 min. The eluted phages were amplified through infection into *Escherichia coli* strain ER2738, followed by purification by precipitation with polyethylene glycol. The amplified and purified phages were titered on Langmuir–Blodgett plates containing X-gal (5-bromo-4-chloro-3-indolyl-β-D-galactoside) and IPTG (isopropyl-β-D-thiogalactopyranoside), and this panning was repeated twice more. The DNA products were then isolated from 12 independent blue plaques and sequenced on ABI Prism 3730xl DNA sequencers (SeqWright, Houston, TX).

Growth and analysis of ZnO nanoparticles: The peptides discovered by the phage display (50 μL, 50 mg mL^{-1}) were mixed with $Zn(NO_3)_2$ solution (50 μL, 10 mg mL^{-1}). After incubating the nanoparticles for 4 days at room temperature, they were collected by centrifugation. After 3 rounds of washing and centrifugation, the nanoparticles were characterized by TEM (JEM 2100 (JEOL) with an acceleration voltage of 200 kV). The samples were prepared by drying one drop of the nanoparticle solution on carbon-coated copper grids.

Received: April 14, 2011
Revised: August 30, 2011
Published online: September 16, 2011

Keywords: bioinorganic chemistry · materials science · nanostructures · peptides · zinc oxide

[1] a) C.-L. Chen, N. L. Rosi, *Angew. Chem.* **2010**, *122*, 1968–1986; *Angew. Chem. Int. Ed.* **2010**, *49*, 1924–1942; b) R. de La Rica, H. Matsui, *Chem. Soc. Rev.* **2010**, *39*, 3499–3509.
[2] M. B. Dickerson, K. H. Sandhage, R. R. Naik, *Chem. Rev.* **2008**, *108*, 4935–4978.
[3] M. Sarikaya, C. Tamerler, A. K. Y. Jen, K. Schulten, F. Baneyx, *Nat. Mater.* **2003**, *2*, 577–585.
[4] a) Y. J. Lee, H. Yi, W.-J. Kim, K. Kang, D. S. Yun, M. S. Strano, G. Ceder, A. M. Belcher, *Science* **2009**, *324*, 1051–1055; b) M. Umetsu, M. Mizuta, K. Tsumoto, S. Ohara, S. Takami, H. Watanabe, I. Kumagai, T. Adschiri, *Adv. Mater.* **2005**, *17*, 2571–2575; c) R. R. Naik, S. J. Stringer, G. Agarwal, S. E. Jones, M. O. Stone, *Nat. Mater.* **2002**, *1*, 169–172; d) S. R. Whaley, D. S. English, E. L. Hu, P. F. Barbara, A. M. Belcher, *Nature* **2000**, *405*, 665–668.
[5] a) M. Okochi, T. Sugita, S. Furusawa, M. Umetsu, T. Adschiri, H. Honda, *Biotechnol. Bioeng.* **2010**, *106*, 845–851; b) N. Yokoo, T. Togashi, M. Umetsu, K. Tsumoto, T. Hattori, T. Nakanishi, S. Ohara, S. Takami, T. Naka, H. Abe, I. Kumagai, T. Adschiri, *J. Phys. Chem. B* **2009**, *114*, 480–486.
[6] a) A. Dey, P. H. H. Bomans, F. A. Müller, J. Will, P. M. Frederik, G. de With, N. A. J. M. Sommerdijk, *Nat. Mater.* **2010**, *9*, 1010–1014; b) F. Nudelman, K. Pieterse, A. George, P. H. H. Bomans, H. Friedrich, L. J. Brylka, P. A. J. Hilbers, G. de With, N. A. J. M. Sommerdijk, *Nat. Mater.* **2010**, *9*, 1004–1009; c) E. M. Pouget, P. H. H. Bomans, J. A. C. M. Goos, P. M. Frederik, G. de With, N. A. J. M. Sommerdijk, *Science* **2009**, *323*, 1455–1458; d) D. Gebauer, A. Völkel, H. Cölfen, *Science* **2008**, *322*, 1819–1822.
[7] a) Z. L. Wang, J. Song, *Science* **2006**, *312*, 242–246; b) M. H. Huang, S. Mao, H. Feick, H. Yan, Y. Wu, H. Kind, E. Weber, R. Russo, P. Yang, *Science* **2001**, *292*, 1897–1899.
[8] R. Monjezi, B. T. Tey, C. C. Sieo, W. S. Tan, *J. Chromatogr. B* **2010**, *878*, 1855–1859.
[9] a) M. Miyauchi, A. Shimai, Y. Tsuru, *J. Phys. Chem. B* **2005**, *109*, 13307–13311; b) X. Y. Kong, Y. Ding, R. Yang, Z. L. Wang, *Science* **2004**, *303*, 1348–1351; c) H. J. Fan, R. Scholz, F. M. Kolb, M. Zacharias, *Appl. Phys. Lett.* **2004**, *85*, 4142–4144.

[10] D. Kisailus, B. Schwenzer, J. Gomm, J. C. Weaver, D. E. Morse, *J. Am. Chem. Soc.* **2006**, *128*, 10276 – 10280.
[11] D. S. Bohle, C. J. Spina, *J. Am. Chem. Soc.* **2009**, *131*, 4397 – 4404.
[12] S.-Y. Lee, X. Gao, H. Matsui, *J. Am. Chem. Soc.* **2007**, *129*, 2954 – 2958.
[13] a) J. Zhang, M. R. Langille, C. A. Mirkin, *J. Am. Chem. Soc.* **2010**, *132*, 12502 – 12510; b) K. G. Stamplecoskie, J. C. Scaiano, *J. Am. Chem. Soc.* **2010**, *132*, 1825 – 1827; c) R. Jin, Y. C. Cao, E. Hao, G. S. Metraux, G. C. Schatz, C. A. Mirkin, *Nature* **2003**, *425*, 487 – 490.
[14] H. Cölfen, M. Antonietti, *Angew. Chem.* **2005**, *117*, 5714 – 5730; *Angew. Chem. Int. Ed.* **2005**, *44*, 5576 – 5591.
[15] J. Zeng, Y. Zheng, M. Rycenga, J. Tao, Z.-Y. Li, Q. Zhang, Y. Zhu, Y. Xia, *J. Am. Chem. Soc.* **2010**, *132*, 8552 – 8553.

